Coulomb excitation of ^{113,115}In†

W. K. Tuttle, III,* P. H. Stelson, R. L. Robinson, W. T. Milner,
F. K. McGowan, S. Raman, and W. K. Dagenhart
Oak Ridge National Laboratory, Oak Ridge, Tennessee 37803
(Received 28 October 1975)

Eight states in ^{113}In and eight states in ^{115}In were observed to be Coulomb excited with α-particle and ^{16}O projectiles. Level energies, spins, $B(E2)$ and $B(M1)$ transition probabilities, and mean lives were obtained. The multiplet formed by $\pi g_{9/2}^{-1} \otimes 2_1^+$(Sn) was found, and the data confirm the coupling strength to be strong. In addition, one extra $\frac{5}{2}^+$ and one extra $\frac{9}{2}^+$ level were seen in each nucleus, along with $E3$ Coulomb excitation of the $\frac{3}{2}^-$ levels. A firm basis for spin-parity assignments was found for all levels observed with the exception of a 1630.5 keV, $\frac{9}{2}^+$ level in ^{113}In. Three of the states in ^{113}In had not previously been observed in Coulomb excitation.

[NUCLEAR REACTIONS ^{113,115}In($\alpha, \alpha'\gamma$) and ^{113,115}In(^{16}O, ^{16}O$'\gamma$) E_α=9.4, 10.0, 10.6 MeV; $E(^{16}\text{O})$=42, 45 MeV; measured E_γ, I_γ, $I_\gamma(\theta)$, Doppler broadening. ^{113,115}In deduced levels, J, π, $B(E2)$, $B(M1)$, $T_{1/2}$. Enriched target.]

I. INTRODUCTION

Having one proton hole in a major proton shell closing at $Z=50$ makes the odd mass In nuclei prime candidates for description by the weak coupling model. Thus these nuclei, particularly ^{115}In, have been the subject of a number of investigations, both theoretical and experimental. The Nuclear Data Sheets[1-4] and some of the more recent articles[5-14] can provide an exhaustive list of references. The latest theoretical results use a unified model to describe the odd In nuclei as ones in which core-coupling states coexist with a deformed rotational band and single particle shell model states.

As part of a program to study intermixing between shell model and collective states in this mass region, as well as to respond to recent theoretical interest, we have performed Coulomb excitation measurements on ^{113,115}In. Four types of experiments were performed as follows: (1) γ-ray yields, (2) γ-γ coincidences, (3) angular anisotropies, and (4) Doppler broadened peak shape lifetimes. The study of ^{115}In served to add more complete and up-to-date information to that already known while at the same time providing a kind of calibration or reference for the ^{113}In work, ^{113}In having not been extensively studied experimentally. Results presented here are the completion of our work reported earlier.[15-17]

II. EXPERIMENTAL PROCEDURE AND RESULTS

A. γ-ray yields and γ-γ coincidences

Coulomb excitation was effected by bombardment with α particle and ^{16}O ions accelerated by the EN tandem Van de Graaff accelerator at Oak Ridge, the ^{16}O ions being used only to observe the Doppler-broadened peak shapes. A natural In foil spot welded onto a 0.013 cm thick Ni backing served as an ^{115}In target. The ^{113}In target was an electrodeposition of target material onto a 0.013 cm thick Ni backing. To eliminate contaminants introduced while being enriched to 96%, the ^{113}In material had to be chemically processed twice to obtain satisfactory spectra. Both targets were thick enough to stop the beam. The γ-ray spectra from the Coulomb excited ^{113,115}In nuclei were measured with three Ge(Li) detectors, rated at 10%, 13%, and 23% efficiencies.

An example of the singles γ-ray spectra is shown in Fig. 1. The spectra observed were fairly clean, showing typical Coulomb excitation contaminant γ rays, and some γ rays due to Fe and Zn in the ^{113}In target. Tables I and II summarize the positions of the levels observed (column 1), the assignment of γ rays (column 2), and the relative intensities of the γ ray depopulating each excited state (column 3). The results of the coincidence measurements are given in Table III, while Figs. 2 and 3 display the level structure deduced.

The coincidence measurements were taken in an event by event mode and processed into a two dimensional 1000×1000 spectrum which was stored on magnetic tape. We were thus able to set gates in either direction on any γ ray of interest. The detectors used were located at 0° and 90° with respect to the beam axis, and 10.6 MeV α particles were used to effect Coulomb excitation.

The $B_{ex}(E2)$ values were extracted from the measured yields by the use of Coulomb excitation the-

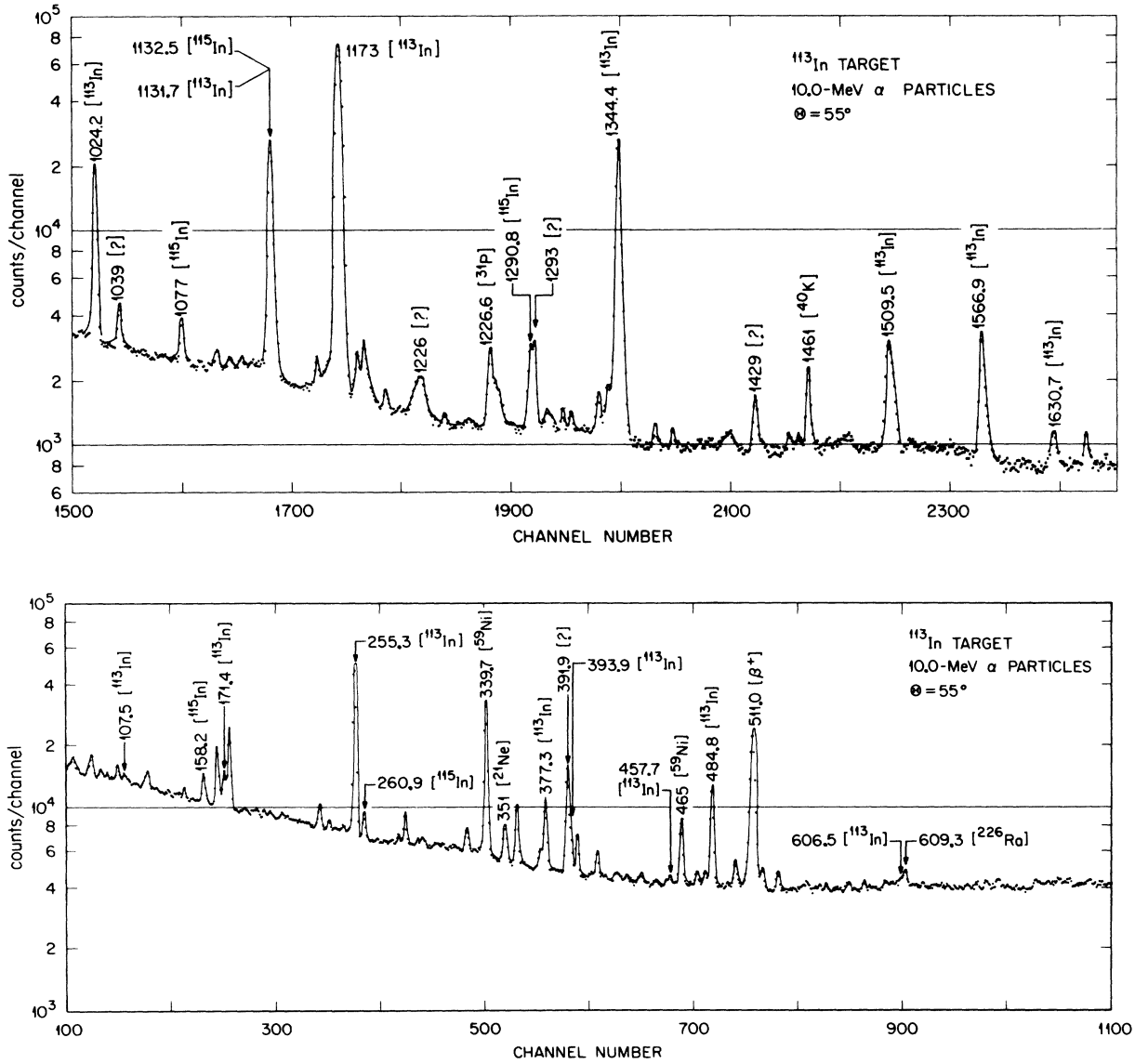

FIG. 1. γ-ray spectrum observed with a 23% Ge(Li) detector when 10.0 MeV α particles Coulomb excited an isotopically enriched ^{113}In target.

ory following a procedure previously described.[18] Results for ^{113,115}In are presented in Table IV, and displayed graphically in Figs. 4 and 5. These values are the average of the results obtained with the Ge(Li) detector located at 55° with respect to the beam, and α-particle beam of energies 9.4, 10.0, and 10.6 MeV. The assigned errors for the absolute $B_{ex}(E2)$ values result from uncertainties in peak area, in the calibrated efficiency of the Ge(Li) detector, and in the stopping power of α particles in In. When appropriate, corrections for internal conversion have been made. States in ^{115}In with $I^\pi = \frac{5}{2}^+$ and $\frac{7}{2}^+$ at energies 933.6 and 1418 keV, respectively, have been seen in the decay of ^{115}Cd^m and therefore might be expected to be Coulomb excited. We saw no evidence for Coulomb excitation of the states and therefore were able to set small upper limits on the $B_{ex}(E2)$ values as shown in Table IV. Additionally, our yield and coincidence measurements found only ~ 60% feeding of the $\frac{3}{2}^-$ level by γ-ray decay in both nuclei, so we propose $E3$ excitation of these levels as given in Table IV. The $B_{ex}(E3)$ values obtained are approximately 2 to 4 times the single particle estimate.

TABLE I. Summary of information obtained from the Coulomb excitation of ^{113}In.

Level (keV)	E_γ (keV)	Branching ratio (%)	$(I^\pi)_i$	$(I^\pi)_f$	$B_d(E2)$ ($\times 10^{-50}\ e^2\mathrm{cm}^4$)	$\frac{B_d(E2)}{B_{s.p.}(E2)}$ [a]	δ	$B_d(M1)$ $[10^{-2}\ (e\hbar/2Mc)^2]$	$(\tau_{cal})_{mean}$ (psec)
1024.2	1024.2	91.0 ± 0.6	$\frac{5}{2}^+$	$\frac{9}{2}^+$	1.26 ± 0.10	3.9	∞	···	5.23 ± 0.42
	377.3	9.0 ± 0.6 [b]	$\frac{5}{2}^+$	$\frac{3}{2}^-$	c	c	d	c	···
1131.7	1131.7	85.1 ± 0.5	$\frac{5}{2}^+$	$\frac{9}{2}^+$	2.67 ± 0.17	8.2	∞	···	1.40 ± 0.10
	484.8	14.0 ± 0.3	$\frac{5}{2}^+$	$\frac{3}{2}^-$	c	c	−0.03 ± 0.05 [c]	c	···
						c	−3.0 ± 0.5 [c]	c	···
	107.5	0.9 ± 0.2	$\frac{5}{2}^+$	$\frac{5}{2}^+$	d	d	$\lvert\delta\rvert \le 0.3$ [e]	d	···
1173.0	1173.0	100	$\frac{11}{2}^+$	$\frac{9}{2}^+$	7.74 ± 0.47	23.8	+0.5 ± 0.2 [f]	28^{+42}_{-13} [f]	0.10 ± 0.06
1344.4	1344.4	97.9 ± 0.1	$\frac{13}{2}^+$	$\frac{9}{2}^+$	3.79 ± 0.23	11.7	∞	···	0.48 ± 0.04
	171.4	2.1 ± 0.1	$\frac{13}{2}^+$	$\frac{11}{2}^+$	2.89 ± 2.89	8.9	+0.03 ± 0.03	48 ± 3	···
1509.5	1509.5	93.5 ± 3.2	$\frac{7}{2}^+$ [g]	$\frac{9}{2}^+$	1.81 ± 0.13	5.6	$-0.5^{-0.2}_{+0.1}$	12^{+5}_{-3}	$0.11^{+0.04}_{-0.02}$
					···	···	−1.5 ± 0.1	1 ± 0.1	0.37 ± 0.04
	377.8	6.5 ± 3.2 [b]	$\frac{7}{2}^+$ [g]	$\frac{5}{2}^+$	d	d	d	d	···
1566.9	1566.9	87.5 ± 0.9	$\frac{9}{2}^+$ [g]	$\frac{9}{2}^+$	1.78 ± 0.12	5.5	−1.5 ± 0.5	1.5 ± 0.5	0.29 ± 0.06
					···	···	$\lvert\delta\rvert \ge 5$	≤0.1	0.42 ± 0.03
	393.9	12.5 ± 0.9	$\frac{9}{2}^+$ [g]	$\frac{11}{2}^+$	d	d	d	d	···
1630.7	1630.7	73.1 ± 4.8	$(\frac{9}{2}^+)$ [g]	$\frac{9}{2}^+$	0.32 ± 0.12	1.0	≥+2.0	≤1.4	$1.3^{+0.4}_{-0.1}$
					···	···	$-0.8^{-\infty}_{+0.4}$	$0.9^{+2.8}_{-0.9}$	$0.65^{+1.0}_{-0.4}$
	606.5	≤1.0	$(\frac{9}{2}^+)$ [g]	$\frac{5}{2}^+$	d	d	d	···	···
	457.7	25.9 ± 4.8	$(\frac{9}{2}^+)$ [g]	$\frac{11}{2}^+$	d	d	d	d	···

[a] $B(E2)_{s.p.} = (e^2/4\pi)(\frac{3}{5})^2(1.2\ \mathrm{fm})^4 A^{4/3} = 32.5\ e^2\mathrm{fm}^4$.
[b] Result of taking $I_\gamma(377.8)/I_\gamma(1509.5) = 0.070 \pm 0.035$, based on ^{113}In coincidence data and ^{115}In analog state.
[c] Spin-parity assignments require transition to be $E1$, $M2$, $E3$, or $M4$, and thus $\delta^2 = \lambda(M2)/(E1)$.
[d] Not measured.
[e] Requirement for $B_d(E2, 107) \le 100 B_d(E2, 1132)$.
[f] Calculated using $\tau = 0.10 \pm 0.06$ psec.
[g] Other spin-parity assignments allowed, see text for discussion.

B. Angular distributions

In Coulomb excitation studies, angular distributions are taken to be of the form

$$W(\theta) = 1 + [\alpha_2]_t g_2 A_2 P_2(\cos\theta) + [\alpha_4]_t g_4 A_4 P_4(\cos\theta),$$

where $[\alpha_2]_t$, and $[\alpha_4]_t$ are the thick-target particle parameters calculated from Coulomb excitation; g_2 and g_4 are the finite angular resolution correction factors, and $P_2(\cos\theta)$ and $P_4(\cos\theta)$ are the Legendre polynomials. The angular distribution coefficients A_2 and A_4 are quantities which, for Coulomb excitation, can be calculated exactly. They are a function of the spin sequence and $E2/M1$ γ-ray mixing ratio. Because the parameter $[\alpha_4]_t$ is usually small, we neglect the P_4 term. Thus the measurement of $R \equiv W(0°)/W(90°)$ determines A_2 and hence the spin sequence(s) and mixing ratios allowed for a particular transition. Results from our measurements are given in Table V. The data were normalized to give the theoretical A_2 for the pure $E2$ transitions in both nuclei. Except for low energy γ rays (≤350 keV) the g_2 and g_4 values were essentially constant, being 0.945 and 0.828, respectively, for the ^{113}In measurements, and 0.968 and 0.899, respectively, for the ^{115}In measurements.

C. Doppler-broadened peak shape lifetimes

A direct determination of the lifetime of a nuclear state can be useful in distinguishing between spins and/or mixing ratios allowed by angular distribution measurements. Because the lifetimes of interest ranged from several psec to about 10^{-2} psec, we were able to obtain this information by interpretation of the shape of a Doppler-broadened γ-ray peak. Most of the work was done with ^{16}O ions as projectiles, although because of experimental difficulties the α-particle data were used in two cases. Typical experimental spectra and calculated shapes are shown in Figs. 6 and 7. Results from our measurements are given in Table VI.

The problems associated with this technique

TABLE II. Summary of results obtained from the Coulomb excitation of ^{115}In.

Level (keV)	E_γ (keV)	Branching ratio (%)	$(I^\pi)_i$	$(I^\pi)_f$	$B_d(E2)$ ($\times 10^{-50}$ e^2cm^4)	$\frac{B_d(E2)}{B_{s.p.}(E2)}$ [a]	δ	$B_d(M1)\times 10^2$ $(e\hbar/2Mc)^2$	$(\tau_{cal})_{mean}$ (psec)
941.4	941.4	89.8 ± 0.4	$\frac{5}{2}^+$	$\frac{9}{2}^+$	0.45 ± 0.03	1.4 ± 0.1	∞	···	21.8 ± 2.0
	344.2	10.2 ± 0.4	$\frac{5}{2}^+$	$\frac{3}{2}^-$	b	b	-0.45 ± 0.30 [b]	b	···
					b	b	-1.5 ± 0.8 [b]	b	···
1077.7	1077.7	83.4 ± 0.4	$\frac{5}{2}^+$	$\frac{9}{2}^+$	3.78 ± 0.20	11.4 ± 0.6	∞	···	1.23 ± 0.07
	480.5	15.6 ± 0.2	$\frac{5}{2}^+$	$\frac{3}{2}^-$	b	b	-0.03 ± 0.05 [b]	b	···
					b	b	-3.0 ± 0.5 [b]	b	···
	136.3	1.0 ± 0.2	$\frac{5}{2}^+$	$\frac{5}{2}^+$	7^{+264}_{-7}	21^{+795}_{-21}	$+0.07 \pm 0.42$	15^{+2}_{-4}	···
					≥271	≥816	$+1.5^{+3.0}_{-1.0}$	4^{+7}_{-4}	···
1132.5	1132.5	100	$\frac{11}{2}^+$	$\frac{9}{2}^+$	8.35 ± 0.43	25.2 ± 1.3	$+0.50 \pm 0.15$ [c]	30^{+53}_{-15}	0.10 ± 0.05
1290.8	1290.8	97.6 ± 0.1	$\frac{13}{2}^+$	$\frac{9}{2}^+$	4.04 ± 0.22	12.2 ± 0.7	∞	···	0.55 ± 0.04
	158.2	2.4 ± 0.1	$\frac{13}{2}^+$	$\frac{11}{2}^+$	$2.3^{+18.1}_{-2.3}$	$6.9^{+54.5}_{-6.9}$	$+0.03 \pm 0.05$	64 ± 4	···
1448.9	1448.9	86.0 ± 0.3	$\frac{9}{2}^+$	$\frac{9}{2}^+$	1.51 ± 0.10	4.5 ± 0.3	$-8.0^{-\infty}_{+7.1}$	$0.03^{+2.7}_{-0.03}$	0.52 ± 0.20
	316.4	14.0 ± 0.3	$\frac{9}{2}^+$	$\frac{11}{2}^+$	5^{+158}_{-5}	15^{+476}_{-15}	$+0.1^{+0.2}_{-0.8}$	37^{+50}_{-12}	···
1463.5	1463.5	94.2 ± 0.4	$\frac{7}{2}^+$ [d]	$\frac{9}{2}^+$	1.20 ± 0.17	3.6 ± 0.5	$-0.30^{-0.35}_{+0.15}$	20^{+60}_{-16}	$0.08^{+0.20}_{-0.06}$
							$-2.5^{-1.5}_{+1.0}$	0.5 ± 0.3	0.81 ± 0.15
	385.8	5.8 ± 0.4	$\frac{7}{2}^+$ [d]	$\frac{5}{2}^+$	$1.7^{+356.0}_{-1.7}$	5^{+1072}_{-5}	-0.05 ± 0.40	70^{+193}_{-55}	···
1486.1	1486.1	78.7 ± 3.2	$\frac{9}{2}^+$	$\frac{9}{2}^+$	0.87 ± 0.09	2.6 ± 0.3	$-0.8^{-0.6}_{+0.5}$ [e]	4^{+12}_{-2} [e]	0.4 ± 0.3
	544.7	3.7 ± 0.6	$\frac{9}{2}^+$	$\frac{5}{2}^+$	16^{+59}_{-7}	48^{+178}_{-21}	∞	···	···
	353.6	17.6 ± 1.2	$\frac{9}{2}^+$	$\frac{11}{2}^+$	289^{+2034}_{-272}	871^{+6127}_{-819}	$+0.8 \pm 0.6$	26^{+236}_{-20}	···

[a] $B_{s.p.}(E2) = e^2/4\pi)(315)^2(1.2\text{ fm})^4(A^{4/3}) = 33.2\ e^2\text{fm}^4$.
[b] Spin-parity assignments require transition to be $E1$, $M2$, $E3$, or $M4$, and thus $\delta^2 = \lambda(M2)/\lambda(E1)$.
[c] Obtained from $\tau_{meas} = 0.10 \pm 0.05$ psec; see text for discussion.
[d] Angular distributions also allow $I^\pi = \frac{9}{2}^+$; see text for discussion.
[e] Calculated from $\tau_{meas} = 0.3 \pm 0.2$ psec.

have been discussed previously.[19] In order to get the best agreement, we doctored the stopping power function for In ions recoiling in In in a manner similar to the phenomenological method discussed by Stokstad *et al.*[20] As calibration points, we used the calculated lifetimes of two unique transitions [$\tau(1291) = 1.27$ psec, $\tau(1078) = 0.55$ psec] in ^{115}In. The resultant stopping power curve for In ions with energies ≥ 2 MeV was 96% of that of Northcliffe and Schilling[21] normalized to the region where the results of Brown and Moak[22] are valid. For lower energies, we used a fairly strong increase in order to quickly stop the recoils. In examining the fits, greater consideration was given to the high-energy tail because of greater confidence in the stopping power at higher recoil energies.

III. DISCUSSION OF LEVEL PROPERTIES

A. 941.4 and 1077.7 keV levels (^{115}In)

The observed branching to the 597.5 keV $\frac{3}{2}^-$ level and the fact that these states are populated by the $E2$ Coulomb excitation process strongly suggests they have $I^\pi = \frac{5}{2}^+$. Our angular distribution and lifetime measurements are consistent with these assignments, including the angular distribution of an observed 136.3 keV transition between the two. Unfortunately, our angular distribution measurement did not accurately determine the mixing ratio for this transition, but we can eliminate the value $\delta_{136} = +1.5^{+3.0}_{-1.0}$ because it would require $B_d(E2,\ 1078 \rightarrow 941) \geq 816$ single particle units (s.p.u.).

B. 1132.5 and 1290.8 keV levels (^{115}In)

For the 1290.8 keV level, our angular distributions allow $I^\pi = \frac{7}{2}^+$ or $\frac{13}{2}^+$. However, for the $I^\pi = \frac{7}{2}^+$ assignment, $\tau_{cal} = 0.31 \pm 0.02$ or 0.026 ± 0.011 psec which does not agree with the measured value of 0.55 ± 0.15 psec. Because for $I^\pi = \frac{13}{2}^+$ $\tau_{cal} = 0.55 \pm 0.04$ psec, the spin-parity of the 1290.8 keV level is taken to be $\frac{13}{2}^+$.

From energy considerations, the 158.2 keV γ ray could be placed between the 1448.9 and 1290.8 keV levels, or between the 1290.8 and 1132.5 keV levels. Our coincidence measurements rule out

TABLE III. Summary of coincidence information obtained from the Coulomb excitation of ^{113,115}In.

Transition energy (keV)	Coincident γ rays (keV) Definite	Possible
	^{113}In	
107.5	377.4, 1024.2	
171.4	1173.0	
255.3	377.4, 484.8	107, 607
377.4	255.3, 484.8, 1131.7	607
393.9	1173.0	
457.7	1173.0	
484.8	255.3, 377.4	1024.2
606.5		377.4, 1024.2
1024.2	107, 607	
1131.7	377.7	
1173.0	171.4, 393.9, 457.7	
	^{115}In	
136.3	260.9, 344.2, 941.4	
158.2	1132.5	
260.9	136.3, 344.2, 385.8, 480.5	
316.4	1132.5	
344.2	260.9, 136.3	
353.6	1132.5	357.7
385.8	260.9, 480.5, 1077.7	136.3
480.5	260.9, 385.8	
544.7	941.4	273.6
941.4	136.3, 544.7	
1077.7	385.8	
1132.5	158.2, 316.4, 353.6	105.8

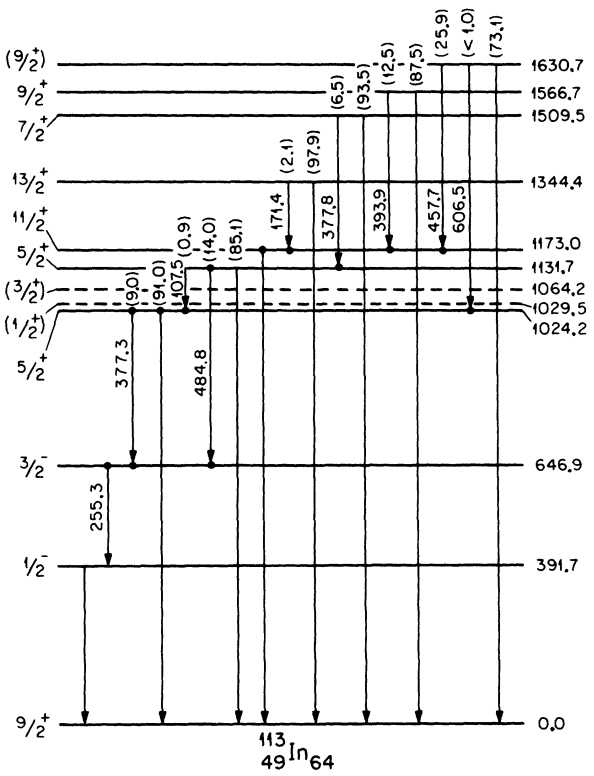

FIG. 2. Level diagram of states observed in the Coulomb excitation of ^{113}In. Branching ratios and coincidences are displayed according to the convention of the Nuclear Data Sheets. Dashed lines indicate low spin positive parity states analogous to those in ^{115}In.

the former possibility. The angular distribution measurements for this transition yield a $\delta_{158} = 0.025 \pm 0.050$ or $-(10^{+10}_{-4})$. The latter assignment is rejected on the basis it requires $B_d(E2, 1291 - 1132) \geq 10^4$ s.p.u.

The angular distribution measurements establish the spin-parity of the 1132.5 keV level as $\frac{7}{2}^+$, $\frac{9}{2}^+$, or $\frac{11}{2}^+$. An assignment of $\frac{11}{2}^+$ is made because it is the only one consistent with the angular distribution of the 158.2 keV γ ray feeding this level from the $\frac{13}{2}^+$ 1290.8 keV level. Since the $\frac{9}{2}^+$ $(E2)$ $\frac{11}{2}^+$ $(E2/M1)$ $\frac{9}{2}^+$ angular distribution is especially flat, the mixing ratio $\delta_{1132} = 0.5 \pm 0.2$ is determined from our lifetime measurement. This value is consistent with the angular distribution measurement where one standard deviation implies $+0.40 \leq \delta_{1132} \leq +5.0$.

C. 1448.9 and 1486.1 keV levels (^{115}In)

For the 1448.9 keV level, our angular distributions of the 1448.9 and 316.3 keV γ rays favor a $I^\pi = \frac{9}{2}^+$ assignment. Our lifetime determination excludes a $\delta \geq +6.5$ for the 1448.9 keV γ ray because it requires $\tau_{1449} \simeq 0.71 \pm 0.05$ psec in contrast to our measured value of $0.15^{+0.10}_{-0.05}$ psec. Unfortunately, the other δ allowed does not quite agree with this lifetime determination. However, because of experimental difficulties, this lifetime had to be deduced from 55° data using α particles to effect Coulomb excitation, making the determination somewhat tenuous. The other alternative is a $\frac{13}{2}^+$ fit to the angular distribution of the 1448.9 keV γ ray which is off by 1.2 standard deviations. However, this spin assignment can be eliminated since the τ value of 1.0 ± 0.1 psec deduced from the $B_{ex}(E2)$ disagrees significantly from the measured value.

For the 1486.1 keV level, our angular distributions of the 1486.1 and 353.6 keV γ rays allow only $I^\pi = \frac{9}{2}^+$, and give a δ_{1486} of $-(0.95^{+\infty}_{-0.35}$ or $+7.5^{+\infty}_{-5.0})$. The latter assignment is eliminated by the lifetime determination of 0.3 ± 0.2 psec. In the summary table we calculated a mixing ratio and $B_d(M1)$ on the basis of this lifetime.

D. 1463.5 keV level (^{115}In)

Our angular distributions of the ground state transition give $I^\pi = \frac{7}{2}^+$ or $\frac{9}{2}^+$. We suggest that the

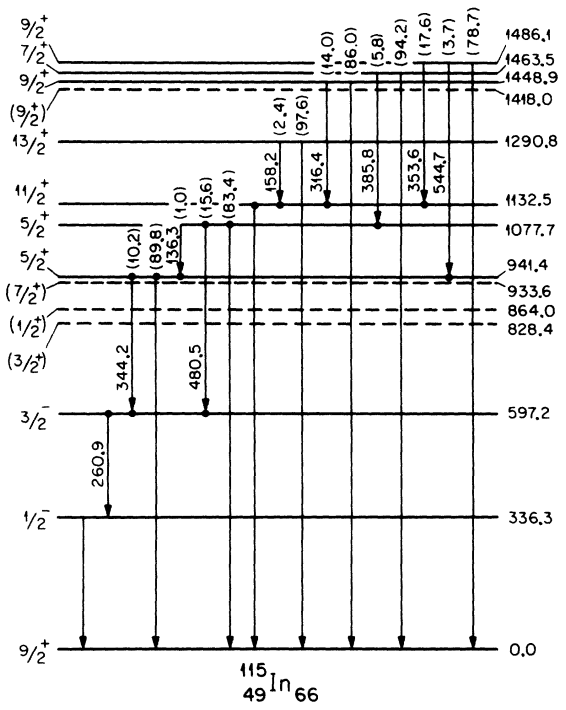

FIG. 3. Level diagram of states observed in the Coulomb excitation of ^{115}In. Branching ratios and coincidences are displayed according to the convention of the Nuclear Data Sheets. Dashed lines indicate states observed in ^{115,115}Cd^{m} decay but not seen in this work.

$\frac{7}{2}^+$ assignment is correct because of the angular distribution of the branching 385.8 keV γ ray from this level and because we observe no branching to the $\frac{11}{2}^+$ 1132.5 keV level in contrast to two other

TABLE IV. Summary of $B_{ex}(E2)$ and $B_{ex}(E3)$ values obtained from the Coulomb excitation of ^{113,115}In.

^{113}In		^{115}In	
Level energy (keV)	$B_{ex}(E2)$	Level energy (keV)	$B_{ex}(E2)$
	(10^{-50} e^2 cm^4)		(10^{-50} e^2 cm^4)
1024.2	0.754 ± 0.062	933.6	<0.006
1131.7	1.60 ± 0.10	941.4	0.272 ± 0.018
1173.0	9.29 ± 0.56	1077.7	2.27 ± 0.12
1344.4	5.30 ± 0.32	1132.5	10.02 ± 0.52
1509.5	1.45 ± 0.10	1290.8	5.65 ± 0.30
1566.9	1.78 ± 0.12	1418	<0.034
1630.7	0.316 ± 0.123	1448.9	1.51 ± 0.10
		1463.5	0.959 ± 0.132
		1486.1	0.871 ± 0.094
	(10^{-75} e^2cm^6)		(10^{-75} e^2cm^6)
646.9	4.82 ± 0.50	597.2	5.73 ± 0.35

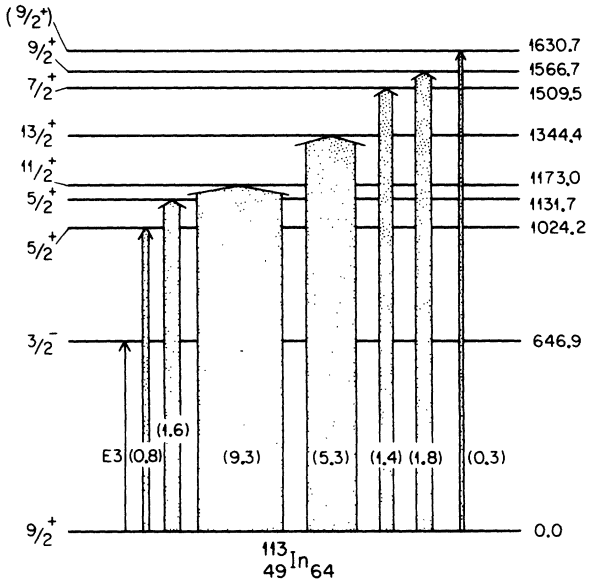

FIG. 4. Level diagram of ^{113}In displaying excitation strengths to the various states of ^{113}In. Widths of arrows are proportional to the $B_{ex}(E2)$. The number in parentheses associated with each arrow is the $B_{ex}(E2)$ in units of 10^{-50} e^2 cm^4.

$\frac{9}{2}^+$ states in this energy region. Furthermore, a $\frac{9}{2}^+$ assignment to the 1463.5 keV level would require $B_d(E2, 1464 \rightarrow 1078) \geq 500$ s.p.u. A direct lifetime determination could not be made.

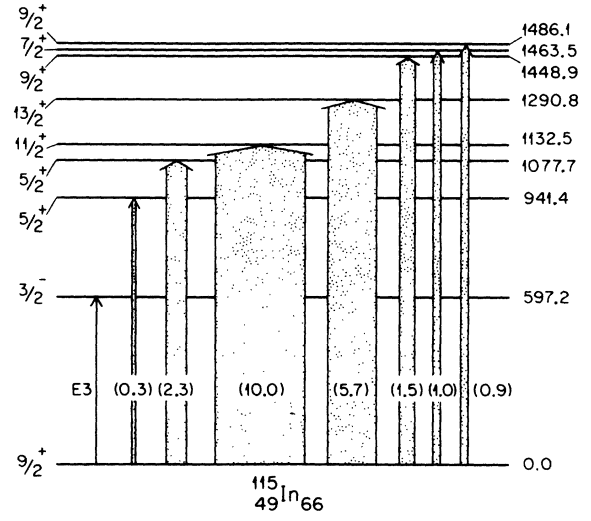

FIG. 5. Level diagram of ^{115}In displaying excitation strengths to the various states of ^{115}In. Widths of arrows are proportional to the $B_{ex}(E2)$. The number in parentheses associated with each arrow is the $B_{ex}(E2)$ in units of 10^{-50} e^2 cm^4.

TABLE V. Summary of γ-ray anisotropy results from the Coulomb excitation of ^{113,115}In.

Level (keV)	E_γ (keV)	$R = W(0°)/W(90°)$	$(\alpha_2)_t$	A_2
		^{113}In		
1024.2	1024.2	1.05 ± 0.02	0.861	+0.04 ± 0.01
1131.7	1131.7	1.01 ± 0.07	0.892	+0.01 ± 0.05
	484.8	0.90 ± 0.03	0.892	−0.08 ± 0.02
1173.0	1173.0	0.98 ± 0.01	0.903	−0.02 ± 0.01
1344.4	1344.4	1.22 ± 0.03	0.945	+0.15 ± 0.02
	171.4	0.89 ± 0.04	0.945	−0.09 ± 0.03
1509.5	1509.5	0.83 ± 0.03	0.979	−0.13 ± 0.02
1566.9	1566.9	1.13 ± 0.04	0.990	+0.08 ± 0.02
1630.7	1630.7	1.06 ± 0.12	1.001	+0.04 ± 0.09
		^{115}In		
941.4	941.4	1.04 ± 0.05	0.833	+0.03 ± 0.04
	344.2	0.80 ± 0.08	0.833	−0.18 ± 0.07
1077.7	1077.7	1.04 ± 0.02	0.877	+0.03 ± 0.02
	480.5	0.90 ± 0.02	0.877	−0.08 ± 0.02
	136.3	1.13 ± 0.12	0.877	+0.10 ± 0.09
1132.5	1132.5	0.97 ± 0.02	0.892	−0.02 ± 0.01
1290.8	1290.8	1.24 ± 0.02	0.933	+0.16 ± 0.02
	158.2	0.88 ± 0.05	0.933	−0.09 ± 0.04
1448.9	1448.9	1.15 ± 0.07	0.967	+0.10 ± 0.05
	316.4	1.14 ± 0.11	0.967	+0.10 ± 0.08
1463.5	1463.5	0.90 ± 0.09	0.970	−0.08 ± 0.07
1486.1	1486.1	1.09 ± 0.09	0.974	+0.06 ± 0.06
	353.6	1.42 ± 0.21	0.974	+0.26 ± 0.13

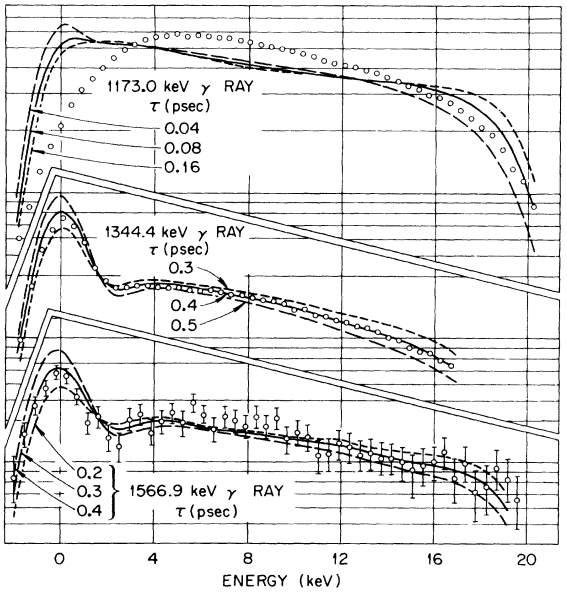

FIG. 6. Doppler-broadened γ-ray peaks observed when ^{113}In was Coulomb excited with ^{16}O projectiles. The detector was located at 0° to the beam direction. The curves are calculated for different values for the mean life τ in psec.

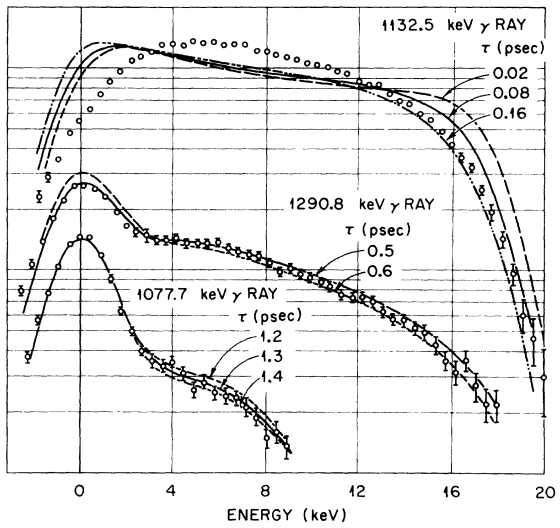

FIG. 7. Doppler-broadened γ-ray peaks observed when ^{115}In was Coulomb excited with ^{16}O projectiles. The detector was located at 0° to the beam direction. The curves are calculated for different values for the mean life τ in psec.

E. 1024.2 and 1131.7 keV levels (^{113}In)

The observed branching to the 646.9 keV $\frac{3}{2}^-$ level, and the fact these states are populated by the $E2$ Coulomb excitation process strongly suggests that these levels have $I^\pi = \frac{5}{2}^+$. For the 1024.2 keV, our angular distribution and lifetime measurements are consistent only with this assignment. The 377.3 keV branch from this level cannot be directly resolved from the 377.8 keV branch of the 1509.5 keV level. To determine the strength of the 377.8 keV transition, we first deduced a branching of (6.5 ± 3.2)% for the 377.8 keV γ ray from the 1509.5 keV level from the ^{113}In co-

TABLE VI. Mean lives of Coulomb excited states in ^{113,115}In obtained by Doppler line shape analysis.

Nucleus	Level (keV)	τ (psec)
^{113}In	1024.2	5.5 ± 1.0
	1173.0	0.10 ± 0.06
	1344.4	0.4 ± 0.1
	1509.5	≤0.3
	1566.9	0.35 ± 0.15
^{115}In	941.4	≥5
	1077.7	1.3 ± 0.2
	1132.5	0.10 ± 0.06
	1290.8	0.55 ± 0.10
	1448.9	$0.15^{+0.10}_{-0.05}$ [a]
	1486.1	0.3 ± 0.2 [a]

[a] Obtained from yield at $\theta_{lab} = +55°$ with 10.0 MeV α particles effecting Coulomb excitation.

incidence measurements. This is similar to the analogous one in ^{115}In. From the intensity of the 1509.5 keV γ ray, we were then able to determine the content of the 377.8 keV transition in the 377 keV peak to be $21 \pm 10\%$. This information was then used in calculating the $B_{ex}(E2)$ for the 1024.2 and 1509.5 keV levels.

Since about 23% of the counts in the 1132 keV peak are due to the 1132.5 keV $\frac{11}{2}^+$ state in ^{115}In, the angular distribution measurement was difficult, and the lifetime measurement impossible. The result of the angular distribution measurement was, however, consistent with the $\frac{5}{2}^+$ assignment of this level.

The observation of a 105.7 keV γ-ray transition between the levels is also consistent with the spin-parity assignments.

F. 1173.0 and 1344.4 keV levels (^{113}In)

For the 1344.4 keV level, our angular distributions give $I^\pi = \frac{7}{2}^+$ or $\frac{13}{2}^+$, and the lifetime measurement eliminates the $\frac{7}{2}^+$ assignment. For the 1173.0 keV level, our angular distributions are consistent with an $I^\pi = \frac{7}{2}^+, \frac{9}{2}^+$, or $\frac{11}{2}^+$ assignment. However, the angular distribution of the 171.4 keV γ ray connecting the two levels permits only an $\frac{11}{2}^+$ assignment for the 1173.0 keV level. Like the ^{115}In analog, the mixing ratio must be taken from the lifetime measurement because of the flatness of the $\frac{9}{2}^+$ $(E2)$ $\frac{11}{2}^+$ $(E2/M1)$ $\frac{9}{2}^+$ distribution.

G. 1509.5, 1566.9, and 1630.7 keV levels (^{113}In)

The angular distribution measurements for the 1509.5 and 1566.9 keV γ rays allow spin-parity assignments of $\frac{7}{2}^+$ or $\frac{9}{2}^+$ for both levels. These assignments cannot be resolved by the lifetime determination. Furthermore, experimental difficulties precluded angular distribution measurements for branching γ rays from these levels. Thus, the assignment of $I^\pi = \frac{7}{2}^+$ for the 1509.5 keV level is based on the observation of the 377.8 keV branch to the $\frac{5}{2}^+$ 1132.5 keV level and on the analogy with ^{115}In. Similarly, the assignment of $I^\pi = \frac{9}{2}^+$ for the 1566.9 keV level is based on the observation of a 393.9 keV branch to the $\frac{11}{2}^+$ 1173.0 keV level and on the analogy with ^{115}In.

The assignment $I^\pi(1630.7\ \text{keV}) = \frac{9}{2}^+$ is based on analogy with ^{115}In.

IV. DISCUSSION OF STRUCTURE

The level structures deduced from this experiment are summarized in Tables I and II, and are displayed graphically in Figs. 2 and 3.

Generally speaking, Coulomb excitation emphasizes collective features which, in a particle-core coupling model for the odd In nuclei, are expected to be dominated by a quintet of states with $I^\pi = \frac{5}{2}^+$ to $\frac{13}{2}^+$ resulting from the coupling of a hole in the $g_{9/2}$ proton shell to the one-phonon vibrational level (2_1^+) of the adjacent even Sn nucleus $(g_{9/2}^{-1} \otimes 2_1^+)$. If the coupling strength is weak (weak coupling model) the sum of the $B_{ex}(E2)$'s for the multiplet should be the same as $B_{ex}(E2, 0^+ \rightarrow 2^+)$ for the adjacent even Sn core, and the $B_d(E2)$ for each member of the multiplet should be the same as $B_d(E2, 2^+ \rightarrow 0^+)$ of the adjacent Sn core. Furthermore, the center of gravity of the multiplet should be the energy of the first 2_1^+ state of the adjacent even Sn core, and there can be no $M1$ component in the ground-state transitions.

A. Ground state and first two excited states

Consideration of the spherical shell model levels leads one to expect the ground state and first excited state of the odd In nuclei to be described by holes in the $1g_{9/2}$ and $2p_{1/2}$ proton orbits. This was established, by the work of Silverburg[23-25] and verified by transfer studies.[11,12,26,27]

The second excited state has been shown[1-4,11,12,26,27] to have $I^\pi = \frac{3}{2}^-$. A state of this nature can arise from a hole in the $2p_{3/2}$ proton orbit or from the coupling of a hole in the $2p_{1/2}$ proton orbit to the one-phonon (2_1^+) state $(P_{1/2}^{-1} \otimes 2_1^+)$ in the adjacent even Sn nucleus. The former state has been calculated[28] to lie about 1.2 MeV, which is the region where the latter could be expected. This being the case, they could interact strongly, so that one is pushed down in energy. Silverburg[25] suggested, and experiments have verified, that the second state is primarily $2p_{3/2}^{-1}$ in character. However, as evidenced by $E3$ excitation, we believe that there is also some collective (possibly $g_{9/2}^{-1} \otimes 3^-$) character to this state.

B. Core-coupled states

The observation of two $\frac{5}{2}^+$ and two $\frac{9}{2}^+$ states poses somewhat of a dilemma. Specifically, which of these are the members of the $g_{9/2}^{-1} \otimes 2_1^+$ multiplet and what is the origin of the others?

In reality, states of the same spin probably contain some component of the multiplet wave function. However, examination of the $B(E2)$ values suggests that the higher lying of the two $\frac{5}{2}^+$ states and the lower lying of the two $\frac{9}{2}^+$ states contain the large component of the $g_{9/2}^{-1} \otimes 2_1^+$ multiplet wave function. For ^{115}In, the choice between $\frac{5}{2}^+$ levels is more apparent than the choice between $\frac{9}{2}^+$ levels. The converse holds for ^{113}In.

Having selected candidates for members of the $g_{9/2}^{-1} \otimes 2_1^+$ multiplet, we are now in a position to further compare the data to the predictions of the

weak coupling model. For ^{115}In, the center of gravity, as given by

$$E_{\text{c.g.}} = \sum_i (2J_i+1)E_i / \sum_i (2J_i+1),$$

is 1287 keV which is in good agreement with the energy (1293 keV) of the 2_1^+ level in ^{116}Sn. The sum of the $B_{\text{ex}}(E2)$ for the multiplet is $20.5 \pm 0.5 \times 10^2\ e^2\text{fm}^4$, which compares with the value $B_{\text{ex}}(E2, 0^+ \to 2^+) = 21.6 \pm 0.6 \times 10^2\ e^2\text{fm}^4$ for ^{116}Sn. Inclusion of the $B_{\text{ex}}(E2)$ for the two "extra" states makes the agreement perfect. However, for ^{113}In, the agreement is not as good. The $E_{\text{c.g.}}$ for the multiplet of ^{113}In and the energy of the 2_1^+ state in ^{114}Sn are, respectively, 1349 and 1300 keV. Furthermore, the sum of the $B_{\text{ex}}(E2)$'s for the multiplet is $19.4 \pm 0.6 \times 10^2\ e^2\text{fm}^4$ which does not agree well with $B_{\text{ex}}(E2, 0^+ \to 2^+) = 23.0 \pm 1.0 \times 10^2\ e^2\text{fm}^4$ for ^{114}Sn. This latter value was obtained from systematics of the $B_{\text{ex}}(E2, 0^+ \to 2^+)$ for the even Sn nuclei as given by Stelson.[29] Inclusion of the "extra" states does not help significantly. Finally, there are other discrepancies from the model, as evidenced in the data for both nuclei. These include appreciable $M1$ components in ground state transitions, uneven distribution of the $B_d(E2)$ strength, and the large

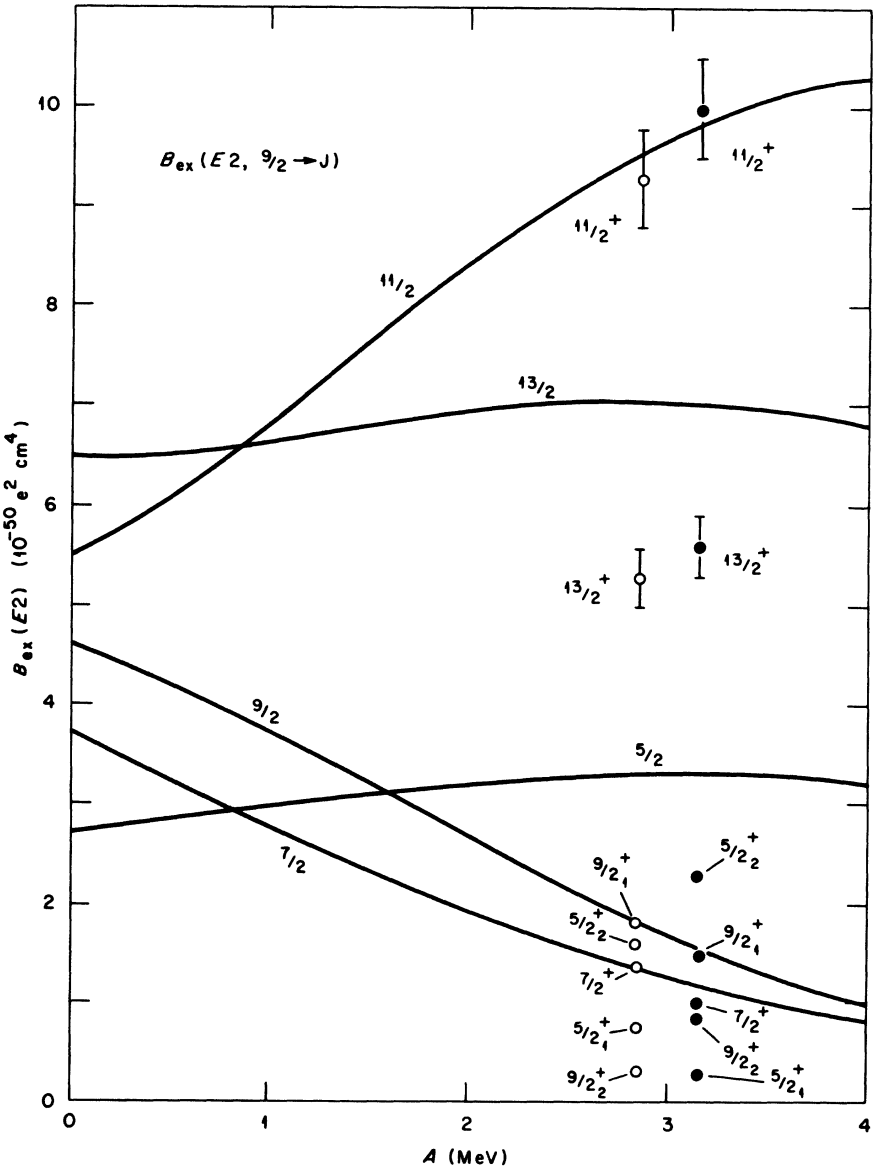

FIG. 8. Plot obtained by Dietrich (Ref. 5) of $B_{\text{ex}}(E2, \frac{9}{2} \to J)$ versus coupling strength for the $g_{9/2}^{-1} \otimes 2_1^+$ (Sn) multiplet in ^{115}In. Data points are this work; the ○ are ^{113}In values, the ● are ^{115}In values.

energy separation of the multiplet compared to the energy of the core 2_1^+ state.

C. Theoretical studies

In order to explain discrepancies such as discussed above, there have been a number of theoretical studies dealing with the structure of the odd In nuclei. We shall compare our results to four of them which are best suited to the nature of our experiment. These comparisons are summarized in Figs. 8 and 9, and in Tables VII and VIII.

The first study we considered was the one by Dietrich.[5] Here a rather simple model for ^{115}In was used in that only the coupling of a $1g_{9/2}$ proton hole to the zero, one, and two quadrupole phonon vibrations of the ^{116}Sn core was considered. The interaction strength A, as defined by

$$\langle(\tfrac{9}{2}^{-1})n'R'J\,|\,H_{\rm int}\,|\,(\tfrac{9}{2}^{-1})nRJ\rangle$$

$$=(-1)^{J-1/2}\begin{Bmatrix} J & \frac{9}{2} & R \\ 2 & R' & \frac{9}{2}\end{Bmatrix}(n'R'\,\|\,\alpha_2^+ + \alpha_2\,\|\,nR)A\,,$$

is treated as a parameter. Plots of energy levels and $B_{\rm ex}(E2)$ strengths were developed as a function of A, the latter of which is reproduced in Fig. 8.

The agreement with experiment for a value of $A\simeq 3.0$ MeV is surprisingly good. The sequence of energy levels is well reproduced except for inversion of the $\frac{11}{2}^+$ and $\frac{5}{2}^+$ states in both nuclei which lie close together, and for ^{113}In, the inversion of the $\frac{7}{2}^+$ and $\frac{9}{2}^+$ states which also are close lying. Increasing the coupling strength will help the latter situation, but at a cost of hurting the over-all agreement. Examination of Fig. 8 shows how well the data fit the predicted $B_{\rm ex}$ $(E2)$ values. For good agreement, one need only consider one of the $\frac{9}{2}^+$ levels, but for the $\frac{5}{2}^+$ levels, the sum of both $B_{\rm ex}$ $(E2)$ is still short of the predicted value. Otherwise, the biggest discrepancy is with the $\frac{13}{2}^+$ level. From this plot it would appear that the coupling strength needs to be a little stronger for ^{115}In than for ^{113}In. To calculate $M1$ transition strengths, another adjustable parameter g_R (core gyromagnetic ratio) is introduced. In Fig. 9 we reproduce Dietrich's[5] plots of $M1$ transition strengths versus A for his "best" value of g_R. The over-all agreement is not as good as that of the $E2$ strengths, but generally speaking it is more difficult to precisely measure $M1$ strenths. Certainly our results are the right order of magnitude and again suggest that the coupling strength is a bit stronger for ^{115}In than for ^{113}In. In Tables VII and VIII we list the values obtained by Dietrich for $E2$ and $M1$ transition strengths using his "best" values of $A=3.0$ MeV and $g_R=0.2$.

A study in the same spirit as Dietrich,[5] but more extensive, was performed by Covello.[8] This study

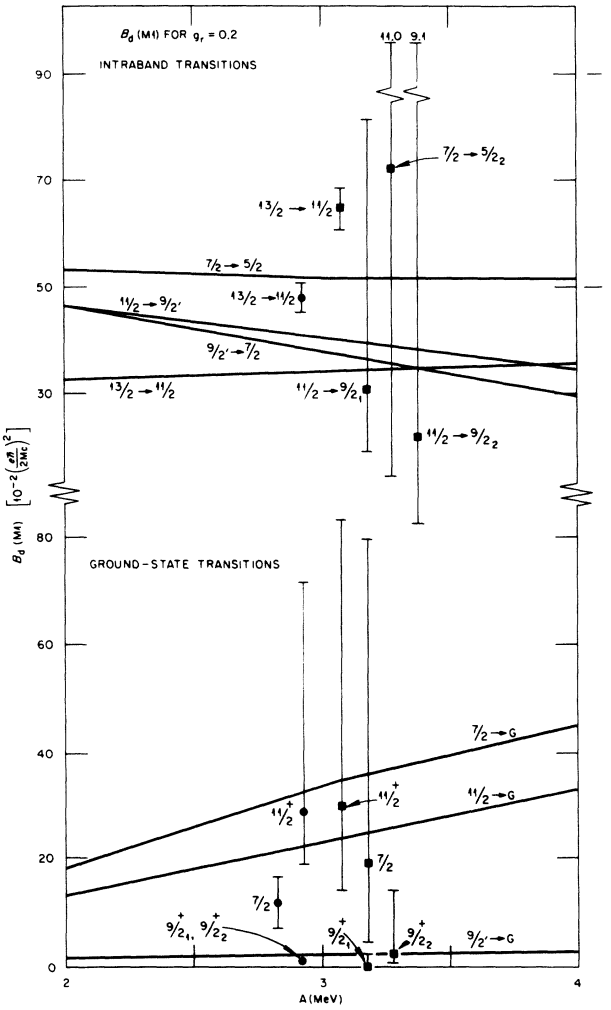

FIG. 9. Plot calculated by Dietrich (Ref. 5) of $B(M1)$ values versus coupling strength for the $g_{9/2}^{-1}\otimes 2_1^+$ (Sn) multiplet in ^{115}In. Data points are this work; the ● are ^{113}In values, the ■ are ^{115}In values.

considered holes in the $1g_{9/2}$, $2p_{1/2}$, $2p_{3/2}$, and $1f_{5/2}$ proton shells coupled to core excitations of up to three quadrupole and one octupole phonons. Also, there were "no adjustable parameters." Such an enlarged model space gives rise to other $\frac{5}{2}^+$ and $\frac{9}{2}^+$ levels, as well as some low spin, positive parity states such as seen in other experimental studies.[1-4,30] The results of Covello's calculations for $E2$ and $M1$ transition strengths are listed in Tables VII and VIII. The over-all level structure determined was similar to that of Dietrich. No additional positive parity states were predicted below 2 MeV, and the electromagnetic properties of the $g_{9/2}^{-1}\otimes 2_1^+$ multiplet are similar.

Sen[6] has performed two types of calculations. First, his "hole-core (hc)" model uses the same model space as Covello,[8] but treats the coupling

TABLE VII. Comparison of calculated and experimental $B_d(E2)$ values of ^{115}In.

$I_i^\pi \to I_f^\pi$	$B_d(E2)$ ($\times 10^{-50}\ e^2\,\mathrm{cm}^4$) Experiment (this work)	Dietrich [a] (Ref. 5)	Sen (Ref. 6)	Covello (Ref. 8)	Abecasis (Ref. 13)
$\frac{5}{2}^+_1 \to \frac{9}{2}^+_g$	0.45 ± 0.03		0.5 [b]		1.4
$\frac{5}{2}^+_2 \to \frac{9}{2}^+_g$	3.78 ± 0.20	6.6 ± 0.7 [c]	4.1 [b]	5.2 [c]	1.7
$\frac{5}{2}^+_2 \to \frac{5}{2}^+_1$	7^{+264}_{-7}				
$\frac{11}{2}^+ \to \frac{9}{2}^+_g$	8.35 ± 0.43	8.1 ± 0.8	6.3 [d]	7.8	8.2
$\frac{13}{2}^+ \to \frac{9}{2}^+_g$	4.04 ± 0.22	5.0 ± 0.5	4.4 [d]	5.0	5.0
$\frac{13}{2}^+ \to \frac{11}{2}^+$	$2.3^{+18.1}_{-2.3}$		1.0 [b]	1.8	2.3
$\frac{9}{2}^+_1 \to \frac{9}{2}^+_g$	1.5 ± 0.1	1.8 ± 0.2 [c]	1.4 [b]	2.1 [c]	2.3
$\frac{9}{2}^+_1 \to \frac{11}{2}^+$	5^{+158}_{-5}		0.5 [b]	1.6 [c]	2.7
$\frac{7}{2}^+ \to \frac{9}{2}^+_g$	1.20 ± 0.17	1.5 ± 0.2	1.9 [d]	1.5	1.0
$\frac{7}{2}^+ \to \frac{5}{2}^+_2$	$1.7^{+256}_{-1.7}$		0.3 [b]	3.4 [c]	
$\frac{9}{2}^+_2 \to \frac{9}{2}^+_g$	0.87 ± 0.09		0.8 [b]		0.0
$\frac{9}{2}^+_2 \to \frac{5}{2}^+_1$	16^{+59}_{-7}				
$\frac{9}{2}^+_2 \to \frac{11}{2}^+$	289^{+2034}_{-272}				

[a] Interpolated from plot using $A = 3.0$ MeV; assume 10% interpolation error.
[b] Result from extended hole-core model, see text for discussion.
[c] Based upon assumption that $\frac{5}{2}^+_2$ and $\frac{9}{2}^+_1$ carry all the strength of the $\frac{5}{2}^+$ and $\frac{9}{2}^+$ members of the $g_{9/2}^{-1} \otimes 2_1^+$ multiplet.
[d] Result from hole-core model, see text for discussion.

TABLE VIII. Comparison of calculated and experimental $B_d(M1)$ values for ^{115}In.

$I_i^\pi \to I_f^\pi$	$B_d(M1)[10^{-2}(e\hbar/2Mc)^2]$ Experiment (this work)	Dietrich [a] (Ref. 5)	Sen (Ref. 6)	Covello (Ref. 8)	Abecasis (Ref. 13)
$\frac{11}{2}^+ \to \frac{9}{2}^+_g$	30^{+53}_{-15}	23 ± 5	18	21	15.9
$\frac{13}{2}^+ \to \frac{11}{2}^+$	64 ± 4	34 ± 7	39	30	30.2
$\frac{9}{2}^+_1 \to \frac{9}{2}^+_g$	$0.03^{+2.7}_{-0.03}$	1.2 ± 0.3 [b]		2 [b]	1.7
$\frac{9}{2}^+_1 \to \frac{11}{2}^+$	37^{+50}_{-12}	48 ± 10 [b]	66	35 [b]	37.5
$\frac{7}{2}^+ \to \frac{9}{2}^+_g$	20^{+60}_{-16}	33 ± 7	25	26	18.2
	0.5 ± 0.3				
$\frac{7}{2}^+ \to \frac{5}{2}^+_2$	70^{+193}_{-55}	51 ± 11 [b]	56	42 [b]	30.5
$\frac{9}{2}^+_2 \to \frac{9}{2}^+_g$	3^{+12}_{-2}				0.6
$\frac{9}{2}^+_2 \to \frac{11}{2}^+$	26^{+236}_{-20}				

[a] Interpolated from plot with $g_R = 0.2$, $A = 3.0$ MeV; assume 20% error from interpolation.
[b] Based upon assumption $\frac{5}{2}^+_2$ and $\frac{9}{2}^+_1$ carry all of the core-coupled strength of the $\frac{5}{2}^+$, $\frac{9}{2}^+$ members of the $g_{9/2}^{-1} \otimes 2_1^+$ multiplet.

strengths and single hole energies as variables. Secondly, his "extended hole-core (ehc)" model attempts to explain discrepancies such as discussed previously by considering the coexistence of a $K = \frac{1}{2}^+$ rotational band built on a deformed Nilsson [431] state with the core-coupled states. This postulate of deformation has previously been used to explain the character of $\frac{1}{2}^+$ and $\frac{3}{2}^+$ levels in odd In nuclei (see Ref. 30 for a recent discussion). With this coexistence, some of the "deformed states" could mix with the core-coupled states, affecting the results as determined by the simpler core-coupled model. Sen treats the interaction matrix for this mixing as a variable, considering only the $\frac{5}{2}^+$ and $\frac{9}{2}^+$ states to be mixed. The results of his calculations are included in Tables VII and VIII; the ehc model results are used whenever possible. This model seems to give a good explanation for the "extra" states, but this may be a result of having more parameters.

A different type of approach to explain the "extra" states and other discrepancies has been explored by Abecasis.[13] Here, in a "generalized semimicroscopic" model, the usual space of the hole phonon coupling model is enlarged by the inclusion of the degrees of freedom associated with the incoherent two-hole–one-particle (2h-1p) modes of excitation. This theory predicts "extra" $\frac{1}{2}^+$, $\frac{3}{2}^+$, $\frac{5}{2}^+$, and $\frac{7}{2}^+$ states. Again, results are listed in Tables VII and VIII.

A comparison of the four theories and the data suggests that to first order, an intermediate coupling strength in a particle-core coupling model provides a good explanation of the features of ^{113,115}In as seen in Coulomb excitation.

V. CONCLUSION

As indicated earlier, the results of our measurements are summarized in Tables I and II, and Figs. 2 and 3. From this, a remarkable similarity between the two nuclei is readily apparent. Their structure is, to first order, explained by a particle-core coupling model with intermediate coupling strength. Differences observed between the structure of the two nuclei are as follows: (1) inversion of the core-coupled $\frac{7}{2}^+$ and $\frac{9}{2}^+$ states, (2) stronger excitation of the lower of the two $\frac{5}{2}^+$ states in ^{113}In vs ^{115}In, and (3) weaker excitation of the higher of the two $\frac{9}{2}^+$ states in ^{113}In vs ^{115}In.

We believe we have contributed a firm experimental basis for spin-parity assignments in both nuclei. Furthermore, in addition to the differences mentioned above, we believe we have posed several important theoretical questions. First, there must be some accounting for $E3$ excitation of the $\frac{3}{2}^-$ levels. Next, there must be some accounting for the nature of the lower of the two $\frac{5}{2}^+$ levels because of the $B_{ex}(E2)$ strength to the one in ^{113}In and because of the observation of a transition between the two. Finally, the low spin positive parity states known to exist in both nuclei must not be appreciably mixed with the core-coupled states. These low spin positive parity states have been described as members of a $K = \frac{1}{2}^+$ rotational band built on a deformed Nilsson [431] state,[30] but we do not see the known transitions from the $\frac{1}{2}^+$ and $\frac{3}{2}^+$ levels to the $\frac{3}{2}^-$ and $\frac{1}{2}^-$ levels in either nuclei, and furthermore can set small upper limits on the $B_{ex}(E2)$ values for the $\frac{7}{2}^+$ and $\frac{9}{2}^+$ members in ^{115}In.

---

*Oak Ridge Associated Universities Graduate Fellow from the University of Tennessee, Knoxville.

†Research sponsored by the U. S. Energy Research and Development Administration under contract with Union Carbide Corporation.

[1]F. E. Bertrand, Nuclear Data 6, 1 (1971).

[2]S. Raman and H. J. Kim, Nucl. Data B6, 39 (1971).

[3]S. Raman and H. J. Kim, Nucl. Data B5, 181 (1971).

[4]S. Raman and H. J. Kim, Nucl. Data B16, 195 (1975).

[5]F. S. Dietrich, B. Herskind, R. A. Naumann, R. E. Stokstad, and G. E. Walker, Nucl. Phys. A155, 209 (1970).

[6]S. Sen, Nucl. Phys. A191, 29 (1972).

[7]V. Sergeev, J. Becker, L. Eriksson, L. Gidefeldt, and L. Holmberg, Nucl. Phys. A202, 385 (1973).

[8]A. Covello, V. R. Manfredi, and N. Assiz, Nucl. Phys. A201, 215 (1973).

[9]H. J. Mang, F. Krmpotic, and S. M. Abecasis, Z. Phys. 262, 39 (1973).

[10]H. J. Kim and R. L. Robinson, Phys. Rev. C 9, 767 (1974).

[11]R. G. Markham and H. W. Fulbright, Phys. Rev. C 9, 1633 (1974).

[12]W. H. A. Hesselink, B. R. Kooistra, L. W. Put, R. H. Siemssen, and S. Y. Van der Werf, Nucl. Phys. A226, 229 (1974).

[13]S. M. Abecasis, O. Civitarese, and F. Krmpotic, Phys. Rev. C 9, 2320 (1974).

[14]W. Dietrich and A. Backlin, Phys. Scr. (to be published).

[15]W. K. Tuttle, III, P. H. Stelson, F. K. McGowan, W. T. Milner, S. Raman, and R. L. Robinson, Bull. Am. Phys. Soc. 19, 1029 (1974).

[16]W. K. Tuttle, III, P. H. Stelson, F. K. McGowan, W. T. Milner, S. Raman, and R. L. Robinson, Bull. Am. Phys. Soc. 20, 686 (1975).

[17]W. K. Tuttle, III, P. H. Stelson, F. K. McGowan, W. T. Milner, S. Raman, and R. L. Robinson, Physics Division Annual Report, 1974, Oak Ridge National Laboratory, ORNL-5025 (unpublished), p. 101.

[18]P. H. Stelson and F. K. McGowan, Phys. Rev. 110, 489

(1958).
[19]P. H. Stelson, W. T. Milner, F. K. McGowan, R. L. Robinson, and S. Raman, Nucl. Phys. A190, 197 (1972).
[20]R. G. Stokstad, I. A. Fraser, I. S. Greenberg, S. H. Sie, and D. A. Bromley, Nucl. Phys. A156, 145 (1970).
[21]L. C. Northcliffe and R. F. Schilling, Nucl. Data A7, 233 (1970).
[22]C. D. Moak and M. D. Brown, Phys. Rev. 149, 244 (1966).
[23]L. Silverburg, Ark. Fys. 20, 341 (1961).
[24]L. Silverburg, Nucl. Phys. 60, 483 (1964).
[25]L. Silverburg, Nucl. Phys. A119, 385 (1968).
[26]M. Conjeaud, S. Harar, and E. Thuriere, Nucl. Phys. A129, 10 (1969).
[27]C. Weiffenbach and R. Tickle, Phys. Rev. C 3, 1668 (1971).
[28]V. R. Pandharipande, Nucl. Phys. A100, 449 (1967).
[29]P. H. Stelson, F. K. McGowan, R. L. Robinson, and W. T. Milner, Phys. Rev. C 2, 2015 (1970).
[30]J. McDonald, B. Fogelberg, A. Bäklin, and Y. Kawase, Nucl. Phys. A224, 13 (1974).

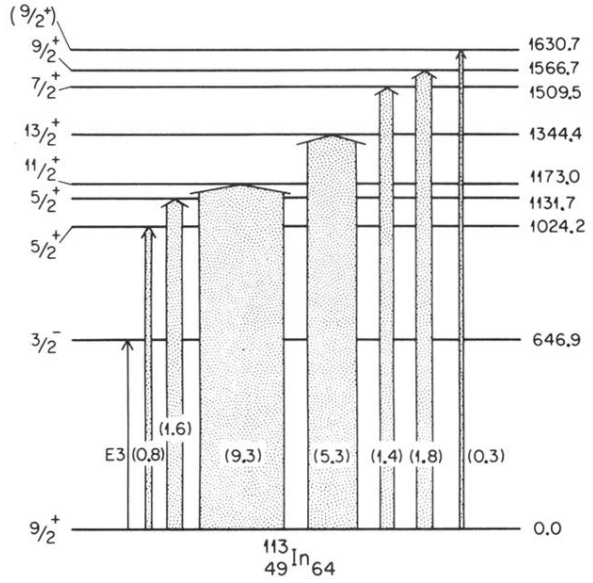

FIG. 4. Level diagram of ^{113}In displaying excitation strengths to the various states of ^{113}In. Widths of arrows are proportional to the $B_{ex}(E2)$. The number in parentheses associated with each arrow is the $B_{ex}(E2)$ in units of $10^{-50}\ e^2\,\mathrm{cm}^4$.

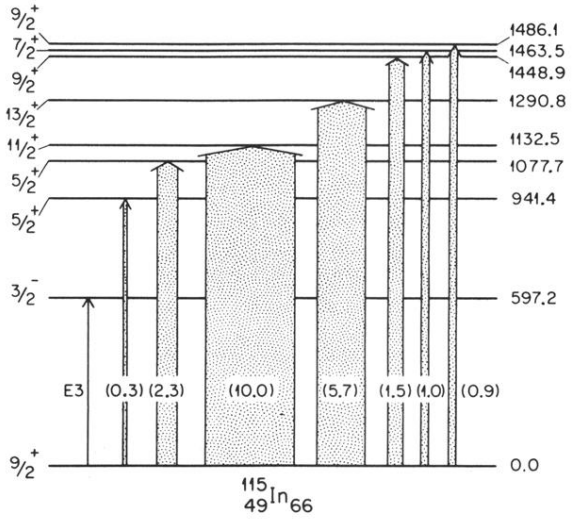

FIG. 5. Level diagram of ^{115}In displaying excitation strengths to the various states of ^{115}In. Widths of arrows are proportional to the $B_{ex}(E2)$. The number in parentheses associated with each arrow is the $B_{ex}(E2)$ in units of 10^{-50} $e^2\,\mathrm{cm}^4$.